

## Runaway electrons in the atmosphere in the presence of a magnetic field

A.V. Gurevich<sup>1</sup>, J. A. Valdivia, G. M. Milikh, and K. Papadopoulos

Departments of Physics and Astronomy, University of Maryland, College Park

**Abstract** This paper generalizes the theory of the electron runaway and runaway discharge to the case of a laminar electric field at an arbitrary angle to the magnetic field and derives the relevant threshold conditions. It is shown that the conditions of the runaway process depend on the angle between the electric and magnetic fields, and the ratio of their magnitudes. In fact, the geomagnetic field hinders the development of runaway breakdown in the atmosphere. This effect has implications for runaway discharges in the atmosphere caused by low-altitude lightning. The runaway discharges manifest themselves as fluxes of  $\gamma$  rays, as previously observed by the detector aboard Compton Gamma Ray Observatory. The geomagnetic field plays a significant role in the runaway discharge due to thunderstorms for heights above 20 km, where the cyclotron frequency of relativistic electrons exceeds their collision frequency. This effect depends on the angle between the electric and magnetic fields. Since the static electric fields from thunderclouds are directed almost vertically, one can expect a significant difference in the properties of high-altitude discharges occurring at equatorial and high-latitude regions.

### 1. Introduction

A new type of electrical air breakdown, called runaway breakdown or runaway discharge, was discussed recently by Gurevich *et al.* [1992] and applied to the preliminary breakdown phase of a lightning discharge. This phase occurs in the cloud vicinity and marks the initiation of the discharge [Uman, 1987]. The important property of the runaway breakdown is that it requires a threshold field of an order of magnitude smaller than the conventional discharge under the same pressure conditions. However, its initiation depends on the presence of seed electrons with energy in excess of tens of keV in the high electric field region. Such energetic electrons are often present in the atmosphere as secondaries generated by cosmic rays [Daniel and Stephens, 1974].

<sup>1</sup>On leave from P.N. Lebedev Institute of Physics, Moscow, Russia.

Copyright 1996 by the American Geophysical Union.

Paper number 96RS02441.  
0048-6604/96/96RS-02441\$11.00

The possibility for influence of cosmic ray secondaries on the lightning discharges was first discussed in a speculative manner by Wilson [1924]. Recently, McCarthy and Parks [1992] attributed X rays observed by aircrafts in association with the effect of thundercloud electric field to runaway electrons. Gurevich *et al.* [1992] presented the first consistent analytic and numerical model of the runaway discharge, and later on, Roussel-Dupre *et al.* [1994] presented its detailed quantitative application to the X ray observations.

The physics of the runaway discharge is based on the concept of electron runaway acceleration in the presence of a laminar electric field [Dreicer, 1960; Gurevich, 1961; Lebedev, 1965]. The runaway phenomenon is a consequence of the long-range, small-angle scattering among charged particles undergoing Coulomb interactions. The scattering cross section decreases with velocity as  $\sigma \sim v^{-4}$ . As a result, for a given electric field value a threshold energy can be found beyond which the dynamic friction cannot balance the acceleration force due to the electric field, resulting in continuous electron acceleration.

Here we review the basic physics of the electron runaway in unmagnetized plasmas, starting with the

electron acceleration in a fully ionized plasma. The cold electrons having mean directed velocity  $v$ , less than the electron thermal speed  $v_T = \sqrt{T/m}$  undergo the dynamical friction force

$$F = m\nu_0 v \quad (1)$$

which is proportional to the electron velocity  $v$ , since at  $v < v_T$  the electron collision frequency  $\nu = \nu_0$  is constant, defined by the electron thermal speed. This is shown in Figure 1 by trace 1. However, for fast electrons having the velocity larger than  $v_T$ , the dynamical friction force reduces when the velocity increases, which is shown by trace 2 in Figure 1

$$F = m\nu(v)v = \frac{4\pi e^4 n}{mv^2} \ln \Lambda, \quad (2)$$

where  $n$  is the electron density and  $\ln \Lambda$  is the Coulomb logarithm. As a result the friction force has a maximum at  $v \simeq v_T$ .

The electric field which balances the dynamical friction force at  $v = v_T$  is known as a Dreicer or critical field:

$$E_D = E_{ci} = \frac{4\pi e^3 n}{T} \ln \Lambda. \quad (3)$$

As illustrated by Figure 1, the dynamical friction can-

not confine the plasma electrons which become runaway, if the electric field  $E$  applied to the plasma is higher than  $E_D$ . On the contrary, if the applied field is less than  $E_D$ , electrons are confined by the dynamical friction. At the same time the electrons acquire relatively small velocity  $v_E$ , directed along  $\mathbf{E}$ . Thus the plasma is heated resistively. However, even in this regime, the friction force cannot confine fast electrons having energy  $\epsilon > \epsilon_c \simeq T(E_D/E)$  (see Figure 1). Such electrons are continuously accelerated by the electric field and run away.

For instance, tokamaks usually operate in the regime of resistive heating, but at some conditions the runaway regime also takes place in tokamaks. A similar situation occurs in the weakly ionized plasma. However, unlike the fully ionized plasma, at low electron velocity the collision frequency  $\nu$  in the weakly ionized gas is determined by the cross section of the electron-neutral collision rather than by the thermal electrons. However, at high electron velocity, when the electron energy exceeds the ionization potential ( $\epsilon > \epsilon_i$ ), the interactions of the fast electrons with the nuclei and atomic electrons obey the Coulomb law. Correspondingly, the dynamical friction force decreases with the electron energy [Bethe and Ashkin, 1953], as shown by equation (2). In this case the value of the critical electric field is given by [Gurevich, 1961]:

$$E_{cn} = \frac{4\pi e^3 Z N_m}{\epsilon_1} k_n. \quad (4)$$

Notice that  $N_m$  is the density of the neutral molecules and  $Z$  is the mean molecular charge, which for air is 14.5, and  $k_n$  is the numerical factor, determined by the type of the neutral gas. In fact, for hydrogen,  $k_n \simeq 0.33$ , and for helium,  $k_n \simeq 0.30$ .

If the electric field is larger than  $E_{cn}$ , the whole bulk electrons are accelerated. If the field is less than  $E_{cn}$ , only a few electrons having energy higher than  $\epsilon_c$  are accelerated:

$$\epsilon > \epsilon_c = \frac{2\pi e^3 Z N_m \ln \Lambda_n}{E}, \quad (5)$$

where  $\Lambda_n \simeq \epsilon_c / Z \epsilon_i$ . These are the runaway electrons in the neutral gas.

We emphasize that the amplitude of the electric field leading to the electron runaway is limited, since only for nonrelativistic electrons does the dynamical friction force drop when the electron energy

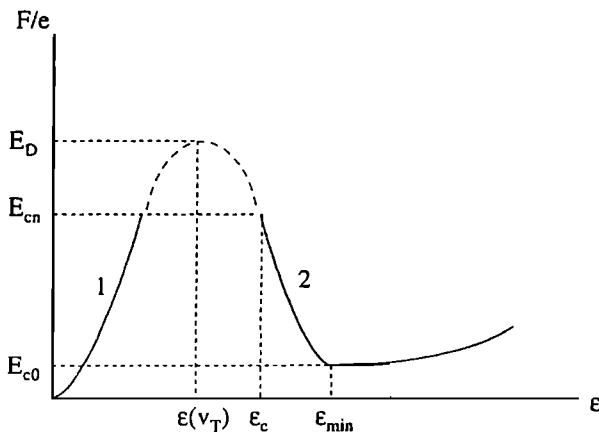


**Figure 1.** Schematic of the dynamical friction force as a function of the electron energy. Trace 1 corresponds to a cold fully ionized plasma ( $v < v_T$ ), and trace 2 corresponds to high-energy plasma electrons. It is valid for any plasmas fully or low ionized. Here  $E_D$  is the Dreicer field, while  $E_{cn}(\epsilon_c)$  and  $E_{c0}(\epsilon_{\min})$  are the critical and minimum runaway fields, respectively.

increases [Bethe and Ashkin, 1953]. For relativistic electrons the friction force reaches its minimum at the energy  $\epsilon \simeq 1.2$  MeV and then slowly (logarithmically) increases with  $\epsilon$  (see Figure 1). The minimum of the friction force  $F_{\min}$  is related to the minimum value of the electric field  $E_{c0}$ , which still generates the runaway:

$$E_{c0} = \frac{4\pi Z e^3 N_m}{mc^2} a. \quad (6)$$

Notice that in the air,  $a \simeq 11.2$ . Therefore, in the air, the runaway electrons could appear in a wide range of electric field  $E_{c0} < E < E_{cn}$ , which spans almost 3 orders of magnitude.

Similar limitation on the electron runaway takes place for the electrons in a fully ionized plasma [Connor and Hastie, 1975]. A detailed discussion of the electron runaway in the air caused by the electric fields due to thunderstorms is presented by McCarthy and Parks [1992].

A new step in the theory of runaway electrons was made by Gurevich *et al.* [1992], who discussed the possibility of producing the avalanche of runaway electrons. The basic idea is that the fast electrons ionize gas molecules, producing a number of free electrons. Some of the secondary electrons have energy higher than the critical energy of runaway. These electrons are accelerated by the electric field and in turn are able to generate fast electrons. The avalanche-like reproduction of fast electrons is accompanied by an exponential increase in the number of thermal secondary electrons, i.e., the electrical breakdown of gas occurs. This kind of runaway breakdown is often called runaway discharge. It has the following main properties: (1) The critical field of the runaway breakdown is an order of magnitude below the threshold of the conventional air breakdown. (2) The runaway discharge has to be triggered by the high energy electron of  $\epsilon > \epsilon_c$ . (3) The runaway discharge develops inside the streamers directed along the electric field [Gurevich *et al.*, 1994]. (4) The runaway discharge is followed by the generation of x- and  $\gamma$ -ray emissions [Roussel-Dupre *et al.*, 1994]. These properties allow us to consider the runaway discharge as the possible mechanism which initializes the lightning discharge during thunderstorms.

Interest in the runaway discharge was recently renewed by the unexpected observations of  $\gamma$ -ray flashes detected by the Compton Gamma Ray Observatory (CGRO) overflying massive thunderstorm regions in the equatorial regions [Fishman *et al.*, 1994]. Early

speculations centered on the runaway discharge driven by the quasi-static fields induced by lightning [Bell *et al.*, 1995; Roussel-Dupre and Gurevich, 1996]. It was shown that the observed  $\gamma$ -ray intensity and spectrum are consistent with bremsstrahlung due to a beam of relativistic electrons with MeV average energy generated at altitudes higher than 30 km. The generation altitude is a key requirement since  $\gamma$  rays generated below 30 km will be absorbed by the atmosphere and will not reach satellite altitudes.

In attempting to apply the concept of runaway breakdown driven by a laminar vertical electric field generated by a lightning discharge at altitudes exceeding 30 km, one is faced with a main difficulty. For such altitudes the mean free path for runaway electrons exceeds the electron gyroradius in the geomagnetic field. As a result, for the large enough angle between the electric field and the geomagnetic field, the previously developed theory of the runaway acceleration is not applicable. This is especially true for the equatorial regions where the vertical electric field due to lightning is predominantly perpendicular to the magnetic field. Note that in  $E \perp B$  geometry, electrons will be accelerated at  $E > B$  if we neglect the dynamical friction. The objective of this paper is to generalize the theory of the runaway acceleration to the case of a laminar electric field at an arbitrary angle to the magnetic field and discuss the relevant threshold conditions for runaway discharge.

In the next section we introduce the equations of motion of the runaway electrons under laminar electric and magnetic fields in the presence of the dynamical friction force. Then we discuss a stationary solution of these equations and obtain the runaway threshold. In section 3 the electron trajectories in momentum space are studied, where we concentrate on the runaway process which occurs in orthogonal electric and magnetic fields. Also in this section the separatrix is obtained, which separates momentum space into two regimes: those electrons which possess trajectories that take them to higher energies and other electrons which possess trajectories leading to zero energy. In section 4 we consider a spreading of runaway discharge stimulated by a high-energy electron. Here the most stress is put on the process which occurs in the parallel electric and magnetic fields. In section 5 we discuss the electron runaway which happens at the arbitrarily angle between the electric and magnetic fields. This is followed by a short discussion and conclusions.

## 2. Motion of Runaway Electrons in the Electric and Magnetic Fields

In the presence of the magnetic field the conditions for electron runaway are different from those described in the previous section. In order to discuss the effects caused by the magnetic field, we will study the motion of fast electrons in the air under the influence of both electric  $\mathbf{E}$  and magnetic field  $\mathbf{B}$ . The latter process is described by the following equation:

$$\frac{d\mathbf{p}}{dt} = e\mathbf{E} + \frac{e}{mc\gamma}(\mathbf{p} \times \mathbf{B}) - \nu\mathbf{p}, \quad \nu = F(p)/p, \quad (7)$$

where  $\mathbf{p}$  is the electron momentum,  $\nu$  is the electron collision frequency, and  $F(p)$  is the dynamical friction force which is a function of electron momentum. For the electrons having energy greater than  $\epsilon \gtrsim 10$  keV, the dynamical friction force due to collisions with the neutral gas is given by [Bethe and Ashkin, 1953]

$$F = \frac{4\pi Ze^4 N_m}{mc^2} \frac{\gamma^2}{\gamma^2 - 1} \times \left\{ \ln \frac{mc^2(\gamma^2 - 1)^{1/2}(\gamma - 1)^{1/2}}{\sqrt{2} I} - \left[ \frac{2}{\gamma} - \frac{1}{\gamma^2} \right] \frac{\ln 2}{2} + \frac{1}{2\gamma^2} + \frac{(\gamma - 1)^2}{16\gamma^2} \right\}, \quad (8)$$

where  $\gamma = (1 - v^2/c^2)^{-1/2}$  is the Lorentz factor and  $I \simeq 80.5$  eV.

For nonrelativistic electrons the dynamical friction force rapidly decreases with the increase of the electron momentum:

$$F = \frac{4\pi Ze^4 N_m m}{p^2} \ln \left( \frac{p^2}{2mI} \right). \quad (9)$$

The dynamical friction force (equation (8)) reaches its minimum value

$$F_{\min} = 10.87 \frac{4\pi Ze^4 N_m}{mc^2} \quad (10)$$

at

$$\gamma_{\min} = 3.42, \quad \epsilon_{\min} = 1.2 \text{ MeV}, \quad p_{\min} = 3.27 mc. \quad (11)$$

$F$  then slowly (logarithmically) increases with  $\gamma$ . As was mentioned in the previous section the value of

$F_{\min}$  just determines the possibility of electrons to runaway in the absence of a magnetic field:

$$E_{co} = F_{\min}/e. \quad (12)$$

We consider now the stationary solution of equation (7)

$$\mathbf{p} = \frac{e E p}{F_D(1 + \omega_c^2/\nu^2)} + \left\{ \hat{e} + \frac{\omega_c^2}{\nu^2} \hat{h} \cos \beta - \frac{\omega_c}{\nu} \hat{e}_\perp \sin \beta \right\}, \quad (13)$$

where  $\hat{e}$ ,  $\hat{h}$ , and  $\hat{e}_\perp$  are the unity vectors directed along  $\mathbf{E}$ ,  $\mathbf{B}$ , and  $\mathbf{E} \times \mathbf{B}$ , respectively, and  $\beta$  is the angle between  $\mathbf{E}$  and  $\mathbf{B}$ . The electron cyclotron frequency is  $\omega_c = eB/mc\gamma$ , and taking into account equation (7), the ratio  $\omega_c/\nu$  can be presented as

$$\frac{\omega_c}{\nu} = \frac{eB}{F} \frac{p}{mc\gamma} = \frac{eB}{F_D} \frac{\sqrt{\gamma^2 - 1}}{\gamma}, \quad (14)$$

Function  $\omega_c/\nu$  determines the effect caused by the magnetic field on the electron motion. Note that this ratio changes rapidly with the height and with the electron energy. We also have to mention that the momentum  $\mathbf{p}$  is given by the solution of equation (13), which is an implicit function, since both the dynamical friction force  $F_D$  and collision frequency  $\nu$  depend on the absolute value of momentum  $\mathbf{p}$  according to equations (7) and (8). Actually, equation (13) represents a set of algebraic equations, which allows us to obtain  $\mathbf{p}$ . To solve this equation set, we consider first the equation for the absolute value of the vector  $\mathbf{p}$ :

$$1 = \frac{eE}{F} \frac{[1 + (\omega_c^4/\nu^4 + \omega_c^2/\nu^2) \cos^2 \beta + \omega_c^2/\nu^2]^{1/2}}{1 + \omega_c^2/\nu^2}. \quad (15)$$

Here  $F$ ,  $\omega_c$ , and  $\nu$  all depend on  $p$ . Note that in order to obtain equation (15), we took into account the following relation

$$\left| \hat{e} + q\hat{h} - q_1\hat{e}_\perp \right| = (1 + q^2 + 2q \cos \beta + q_1^2 \sin^2 \beta)^{1/2}, \quad (16)$$

where  $q$  and  $q_1$  are certain functions.

We solve equation (15) to obtain the absolute value of momentum  $p$ . Substitute it then into the right side of equation (13), and we obtain the desired stationary solution in the form  $p_{st} = p_{st}(E, B, N_m)$ . Note that if the electric field is significantly higher

than the critical field

$$E \geq 2E_{c0} \tag{17}$$

the minimum electron kinetic energy required for runaway is  $\epsilon_{st} < mc^2$ . Therefore, in this case, it is convenient to use the nonrelativistic expression (9) for the dynamical friction force.

In the absence of a magnetic field ( $B = 0$ ), equation (15) determines two stationary points at  $E > E_{c0}$ . The first of these points is reached at  $p_{st} < p_{min}$ , given by equation (12). This is an unstable point. It means that the electrons having  $p < p_{st}$  are decelerated, while the electrons with  $p > p_s$  are accelerated and run away. The limit mentioned above is correct for the momentum parallel to the electric field. If the initial electron momentum possesses a component orthogonal to  $\mathbf{E}$ , a separatrix appears which separates the runaway electrons from those losing their energy [Gurevich et al., 1992; Roussel-Dupre et al., 1994].

The same picture is correct if the constant magnetic field  $\mathbf{B}$  exists which is parallel to  $\mathbf{E}$ . However, if the component of  $\mathbf{E}$  orthogonal to  $\mathbf{B}$  appears, it can significantly change the above picture.

Let us consider a case when  $\mathbf{E} \perp \mathbf{B}$ . We first introduce the dimensionless parameters

$$\delta_0 = E/E_{c0}, \quad \eta_0 = B/E_{c0} \tag{18}$$

Using these parameters and taking into account equation (14) we rewrite equation (15) as

$$1 = \frac{\delta_0}{\Phi(\gamma)} \frac{1}{\{1 + \eta_0^2/\Phi^2(\gamma)[1 - 1/\gamma^2]\}^{1/2}}, \tag{19}$$

where  $\Phi(\gamma) = F_D(\gamma)/eE_{c0}$ . From equation (19) we obtain that

$$\delta_0^2 = \Phi^2(\gamma) + \eta_0^2(1 - 1/\gamma^2), \tag{20}$$

$$\Phi(\gamma_{min}) = 1, \quad \gamma_{min} = 3.42.$$

Relation (20) defines the value of  $\gamma_{st}$  and correspondingly  $p_{st}$  for different parameters  $\delta_0$  and  $\eta_0$ . We find next the dimensionless critical field  $\delta_{c0}$  as the minimum value of  $\delta_0(\gamma)$  which still allows solution of equation (20). Equating the derivative  $d\delta_0^2/d\gamma$  to zero, we find

$$\eta_0^2 = -\gamma^3\Phi(\gamma) \frac{d\Phi(\gamma)}{d\gamma}. \tag{21}$$

We combine equations (20) and (21) and find

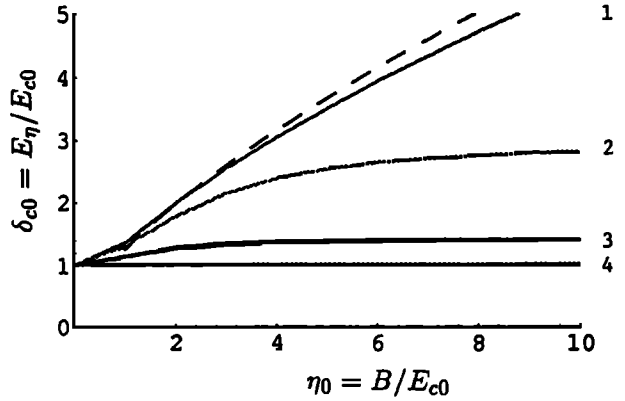


**Figure 2.** Threshold electric field  $\delta_{c0}$  versus magnetic field  $\eta_0$  obtained from equations (21) and (22) for  $\beta = 90^\circ, 70^\circ, 45^\circ,$  and  $10^\circ$  (curves 1, 2, 3 and 4, respectively). The dashed trace shows analytical approximation (24) valid at  $\beta = 90^\circ$  for the nonrelativistic case.

$$\delta_{c0}^2 = -\gamma(\gamma^2 - 1)\Phi(\gamma) \frac{d\Phi(\gamma)}{d\gamma} + \Phi^2(\gamma). \tag{22}$$

Equation (22), together with equation (21), determine in an implicit form the dimensionless critical field  $\delta_{c0}$  and minimum value  $\gamma_c$ , depending on the dimensionless magnetic field  $\eta_0$ . In fact, in the absence of a magnetic field ( $\eta_0 = 0$ ), we obtain from equations (20) and (21) that  $\delta_{c0} = 1$ , and  $\gamma_c = \gamma_{min} = 3.42$ . The dependence of  $\delta_{c0}$  on  $\eta_0$  is shown in Figure 2. This figure reveals that the critical electric field  $\delta_{c0}$  gradually increases as the magnetic field  $\eta_0$  rises.

We find now the asymptotic form for  $\delta_{c0}$  at high values of  $\eta_0$ . In order to do so we take into account that at high  $\eta_0$ , the value  $(v/c)^2 \ll 1$ , so the non-relativistic dynamical friction force given by equation (9) can be applied. Therefore the function  $\Phi(\gamma)$  is rewritten as

$$\Phi(\gamma) = \Phi_0 \frac{\gamma^2}{\gamma^2 - 1}, \quad \Phi_0 \simeq 0.913. \tag{23}$$

Using equations (21)-(23), we obtain that

$$\delta_{c0} = \frac{\sqrt{3} \Phi_0^{1/3}}{2^{1/3}} \eta_0^{2/3}, \quad \frac{\gamma_c^2 - 1}{\gamma_c^2} = \frac{\sqrt{3} \Phi_0}{\delta_{c0}}. \tag{24}$$

The asymptote given by equation (24) is shown by a dashed trace in Figure 2.

The above discussion was focused on an instructive case when  $\mathbf{E} \perp \mathbf{B}$ . However, equation (15) allows

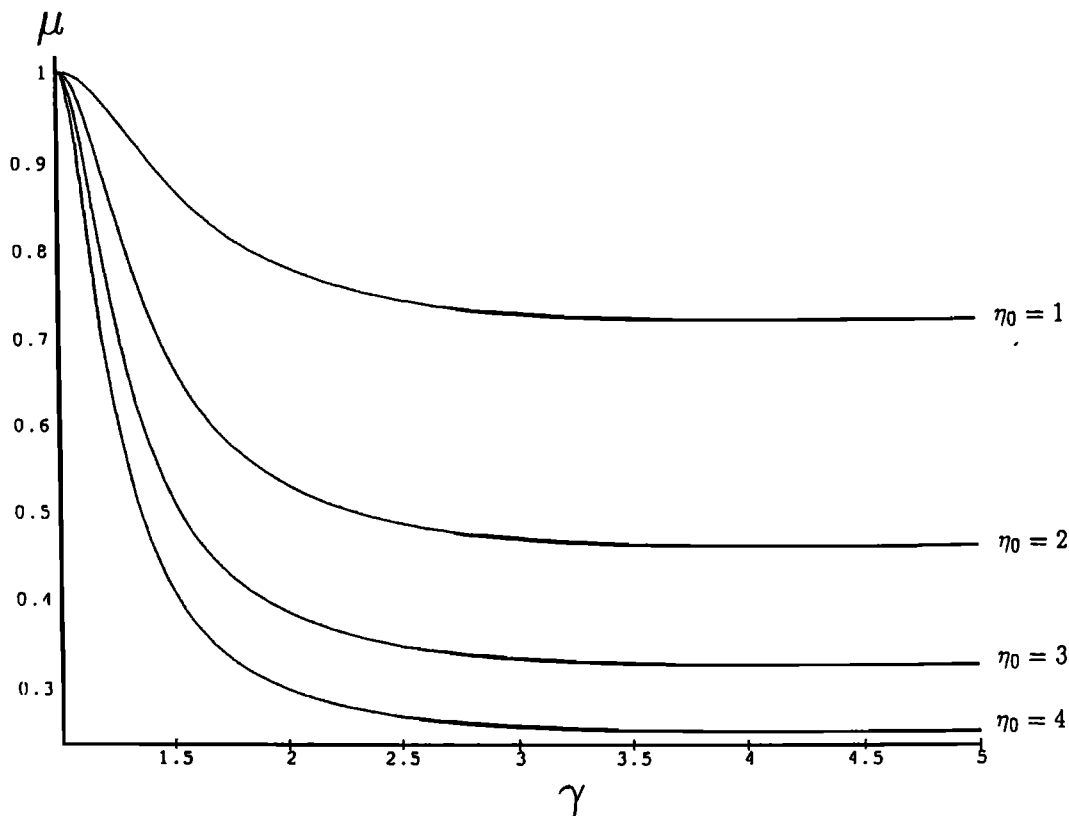


**Figure 3.** Cosine of the angle between the direction of the magnetic field and the electron velocity given as a function of the Lorentz factor  $\gamma$ , drafted for the different values of the normalized magnetic field  $\eta_0$ .

us to obtain the critical electric field  $\delta_{c0}$  as a function of the magnetic field  $\eta_0$  for an arbitrary angle  $\beta$  between the directions of the electric and magnetic fields. This is shown in Figure 2. In fact, for  $\beta \leq 45^\circ$  the critical electric field practically does not depend on the value of the magnetic field, which resembles the runaway as it occurs in the absence of the magnetic field and is driven by the  $E_{\parallel}$  component of the electric field.

Note that the runaway electron moves at an angle  $\alpha$  to the direction of the electric field, where the angle  $\alpha$  is obtained from equation (13). In fact, for  $\mathbf{E} \perp \mathbf{B}$ , i.e.,  $\beta = 90^\circ$ , it acquires the following form:

$$\mu = \cos \alpha = \left( 1 + \frac{\eta_0^2(\gamma^2 - 1)}{\gamma^2 \Phi^2(\gamma)} \right)^{-1/2}. \quad (25)$$

Figure 3 shows that electrons having low energy ( $\gamma \simeq 1$ ) move almost parallel to the direction of the electric field. This is due to the fact that at low electron energy the electron collision frequency is much

higher than the cyclotron frequency  $\omega_c$ , and thus the effect caused by the magnetic field on the electron motion is not significant. When the electron energy increases, the electron collision rate reduces rapidly. It leads to a deflection of the electron velocity from the direction of the electric field. If the magnetic field increases, the angle  $\alpha$  gradually tends to  $\pi/2$ , i.e., in a strong magnetic field, relativistic electrons start drifting in the  $\mathbf{E} \times \mathbf{B}$  direction.

### 3. The Electron Runaway Basin Boundary

#### 3.1. Equations of the Electron Motion

We now study the equation of the electron motion (equation (7)) in order to obtain the separatrix which separates momentum space into two regimes: those electrons which possess trajectories that take them to higher energies and other electrons which possess trajectories leading to zero energy. Using the dimensionless variables  $\delta_0$  and  $\eta_0$  defined by equation (18), equation (7) is presented as

$$\frac{d\tilde{p}_x}{d\tau} = \delta_0 + \frac{\eta_0}{\gamma} \tilde{p}_y \sin \beta - \frac{\Phi(\gamma)}{\sqrt{\gamma^2 - 1}} \tilde{p}_x, \quad (26a)$$

$$\frac{d\tilde{p}_y}{d\tau} = -\frac{\eta_0}{\gamma} \tilde{p}_x \sin \beta + \frac{\eta_0}{\gamma} \tilde{p}_z \cos \beta - \frac{\Phi(\gamma)}{\sqrt{\gamma^2 - 1}} \tilde{p}_y, \quad (26b)$$

$$\frac{d\tilde{p}_z}{d\tau} = -\frac{\eta_0}{\gamma} \tilde{p}_y \cos \beta - \frac{\Phi(\gamma)}{\sqrt{\gamma^2 - 1}} \tilde{p}_z, \quad (26c)$$

$$\gamma = \sqrt{1 + \tilde{p}_x^2 + \tilde{p}_y^2 + \tilde{p}_z^2}, \quad (26d)$$

where we use the dimensionless momentum  $\tilde{p}_{x,y,z}$  by normalizing the conventional momentum over  $mc$ ;  $\tau$  is the dimensionless time

$$\tau = t/t_0, \quad t_0 = \frac{m^2 c^3}{4\pi e^4 Z N_m a} \simeq 2.1 \times \left( \frac{10^{11} \text{cm}^{-3}}{N_m} \right), \quad (27)$$

and  $\beta$  is the angle between the directions of the electric and magnetic fields. Here the electric field goes along the  $x$  axis, while the magnetic field is located in the  $x$ - $z$  plane.

Equations (26a)–(26d) were integrated numerically. Results of the computation are discussed starting with two limit cases:  $\mathbf{E} \perp \mathbf{B}$ , i.e.,  $\beta=90^\circ$ , and  $\mathbf{E} \parallel \mathbf{B}$ , i.e.,  $\beta=0$ .

### 3.2. Electron Runaway in Perpendicular Electric and Magnetic Fields

In this case the momentum is fading along the axes  $z$ , so essentially, electrons are moving in the  $x$ - $y$  plane. At low magnetic field  $\eta_0 < \delta_0$ , two kind of trajectories occur depending on the initial conditions. An electron having low initial energy loses its energy and eventually stops, while the electron having high enough initial energy runs away along the trajectory almost linear in  $\tilde{p}_x, \tilde{p}_y$  space and gains the energy. This regime resembles runaway as it happened in the absence of a magnetic field.

The picture changes when the magnetic field increases so that  $\eta_0 \geq \delta_0$ . In this case, three different types of trajectories occur, depending on the initial conditions, as shown in Figure 4 along with the corresponding temporal evolution of the electron kinetic energy.

In some cases an energetic electron starts from a point marked by a cross in the  $\tilde{p}_x, \tilde{p}_y$  plane and then rapidly loses its energy and eventually stops (Figures

4a and 4b). In other cases the electron starts at a point marked by a cross and then moves along the spiral trajectory, while the electron kinetic energy rapidly increases (at  $t \simeq t_0$ ) and then reaches its steady state value after making several oscillations (Figures 4c and 4d). This regime is strongly different from what happened in the absence of a magnetic field, since in the absence of a magnetic field the runaway electron gains a very high energy, while in the  $\mathbf{E} \perp \mathbf{B}$  field the steady state is reached at a much smaller electron energy.

We describe also the third kind of trajectory when the electron moves along the spiral trajectory, loses its energy, and eventually stops (Figures 4e and 4f). This happens when the  $\tilde{p}_y$  momentum component reaches such negative value that the first and second terms in the right-hand side of Equation (26a) cancel each other ( $\tilde{p}_y \simeq -\gamma\delta_0/\eta_0$ ), leading to the exponential temporal decay of the  $\tilde{p}_x$  component. This is followed by the temporal decay of the  $\tilde{p}_y$  component, coming from equation (26b). However, when relativistic electrons gain and lose energy, they can generate bremsstrahlung emission and might produce secondary runaway electrons.

We proceed by defining the separatrix as a line in the  $v_x^0 = v_x(t=0)$  and  $v_y^0 = v_y(t=0)$  plane which separates the initial electron velocities leading to the runaway regime from those leading to the electron deceleration in a given electric and magnetic field. This is shown in Figure 5a, calculated for the normalized electric field  $\delta_0 = 5$ , and for a few different values of a normalized magnetic field ( $\eta_0 = 6.0, 6.5, 7.0$ , and  $7.5$ ). For each of these cases the runaway process occurs for  $v_x^0, v_y^0$  located inside the domain bounded by the corresponding runaway separatrix. Note that when the applied magnetic field increases, the region of runaway shrinks. Finally,  $\eta_0$  reaches the maximum value  $\eta_{c0}(\delta_0)$  when runaway ceases. In fact, at  $\delta_0 = 5$  the runaway ceases at  $\eta_0 = 7.8$ , which is in considerable agreement with the critical value  $\delta_{c0}(\eta_0 = 7.8) = 4.9$  (see Figure 2), found above by using some simplifications.

Note that a primary runaway electron is able to produce a secondary electron which also runs away if the kinetic energy of the primary electron is at least twice that required for runaway. This is the condition of the runaway breakdown [Gurevich *et al.*, 1994]. The separatrix of runaway breakdown is obtained as it was done for the runaways but using an additional condition that the steady state kinetic energy of the runaway electron is twice as large as its initial value.

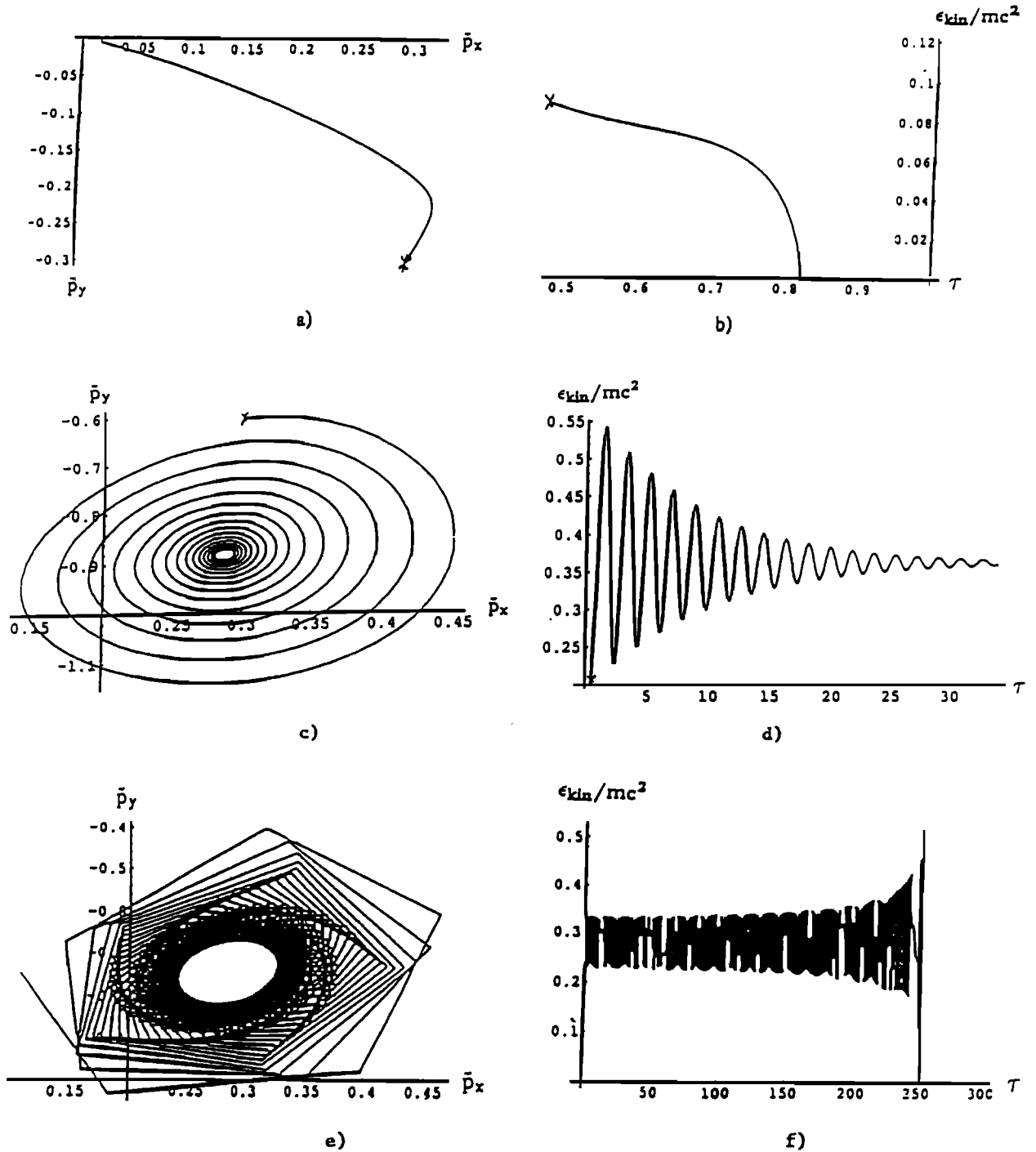


**Figure 4.** (a) Electron trajectory in the  $\bar{p}_x$ ,  $\bar{p}_y$  plane, along with (b) the temporal evolution of its kinetic energy, obtained for  $\mathbf{E} \perp \mathbf{B}$  at  $\delta_0 = 5$ ,  $\eta_0 = 7$  and for the initial values  $\bar{p}_x^o = 0.3$ ,  $\bar{p}_y^o = -0.3$ . (c) and (d) Trajectory obtained at  $\bar{p}_x^o = 0.3$ ,  $\bar{p}_y^o = -0.6$ . (e) and (f) Trajectory obtained at  $\delta_0 = 5$ ,  $\eta_0 = 7.5$ , and for the initial values  $\bar{p}_x^o = 0.3$ ,  $\bar{p}_y^o = -0.65$ .



This is shown in Figure 5b for the same values of electric and magnetic fields as in Figure 5a. Since the requirements for runaway breakdown are stronger than for just runaway, the corresponding domain is smaller than that for the runaways. In fact the runaway discharge developed at  $\delta_0=5$  ceases if  $\eta_0>7$ .

#### 4. Spreading of the Runaway Discharge in the Presence of a Magnetic Field

We consider now the runaway discharge stimulated by a seed high-energy electron. In the absence of the magnetic field the runaway discharge spreads inside a cone stretched along the direction of the electric field [Gurevich et al., 1994]. Below we discuss how the magnetic field affects the structure of the runaway discharge and the dynamics of its spreading. We concentrate mainly on the case when the electric and magnetic fields are parallel to each other. The motion of runaway electrons is studied in the spheric coordinate frame, in which both E and B vectors are directed along the x axis, and the electron momentum evolves with an angle  $\theta$  with the x axis, while its projection on the z-y plane evolves with an angle  $\varphi$  with the y axis. In this frame, equations (26a)–(26d) can be represented as

$$\begin{aligned} \frac{d\tilde{p}}{d\tau} &= \gamma [\delta_0\mu - \Phi(\gamma)], \\ \frac{d\mu}{d\tau} &= \delta_0\gamma \frac{1 - \mu^2}{\tilde{p}}, \\ \frac{d\varphi}{d\tau} &= \eta, \end{aligned} \tag{28}$$

where  $\mu = \cos \theta$  and  $\tilde{p} = \sqrt{\tilde{p}_y^2 + \tilde{p}_z^2}$ . The electron trajectory in the  $\tilde{p}, \mu$  plane is described by the following equation:

$$\frac{d\tilde{p}}{d\mu} = \frac{1}{\delta_0(1 - \mu^2)} [\delta_0\mu - \Phi(\gamma)]. \tag{29}$$

Correspondingly, the separatrix which separates accelerating and decelerating electron trajectories in this plane is defined by the equation

$$\Phi(\gamma) = \delta_0\mu. \tag{30}$$

Figure 6 shows the minimum initial electron energy required for runaway as a function of initial electron direction  $\mu$ . This is calculated for a few different

values of normalized electric field ( $\delta_0 = 2, 3, 4, 5,$  and  $10$ ). Shown by a dashed trace is the same separatrix obtained by Gurevich et al. [1994] for  $\delta_0 = 2$ , and by the relativistic effects.

We consider next the diffusion of runaway electrons which occurs in a plane perpendicular to E, and is caused by the fact that secondary electrons appear at an arbitrarily angle. As a result of this diffusion the runaway discharge caused by a single seed electron acquires a conical shape as shown by Gurevich et al. [1994] in the absence of a magnetic field.

The runaway electron possesses two velocity components in the y, z plane:

$$\begin{aligned} \tilde{v}_z &= \frac{d\tilde{z}}{d\tau} = \frac{\tilde{p}}{\gamma} \sqrt{1 - \mu^2} \sin \varphi, \\ \tilde{v}_y &= \frac{d\tilde{y}}{d\tau} = \frac{\tilde{p}}{\gamma} \sqrt{1 - \mu^2} \cos \varphi, \end{aligned} \tag{31}$$

where  $\tilde{y}, \tilde{z}$  are given in the dimensionless units  $\tilde{y} = y/ct_0, \tilde{z} = z/ct_0$ , and  $t_0$  is defined by equation (27). In order to obtain the mean free path of the runaway electron, we integrate equation (31) using equation (28) and take into account that the secondary electron which is born at the spot  $\mu_0$  close to the separatrix propagates freely until the spot  $\mu_1$ , when its energy increases to twice its initial value. Therefore we have

$$\begin{aligned} r_\mu^2 &= (\bar{\Delta}\tilde{y})^2 + (\bar{\Delta}\tilde{z})^2, \\ \Delta\tilde{y} &= \int_{\mu_0}^{\mu_1} \frac{\tilde{p}^2}{\delta_0\sqrt{1 + \tilde{p}^2}} \frac{\sin(\varphi_0 + \eta\tau)}{\sqrt{1 - \mu^2}} d\mu, \\ \Delta\tilde{z} &= \int_{\mu_0}^{\mu_1} \frac{\tilde{p}^2}{\delta_0\sqrt{1 + \tilde{p}^2}} \frac{\cos(\varphi_0 + \eta\tau)}{\sqrt{1 - \mu^2}} d\mu, \end{aligned} \tag{32}$$

where  $\varphi_0 = \varphi(\tau = 0)$  and the bar shows averaging over  $\varphi_0$ .

The characteristic time  $\Delta\tau$  needed for an electron to propagate from point  $\mu_0$  to  $\mu_1$  can be obtained from equation (28). The diffusion coefficient D is then found to be

$$D_\perp = r_\mu^2/2 \Delta\tau, \quad \Delta\tau = \int_{\mu_0}^{\mu_1} \frac{\tilde{p}}{\delta_0\sqrt{1 + \tilde{p}^2}(1 - \mu^2)} d\mu \tag{33}$$

The diffusion coefficient found from equations (32) and (33) is shown in Figure 7 for different val-

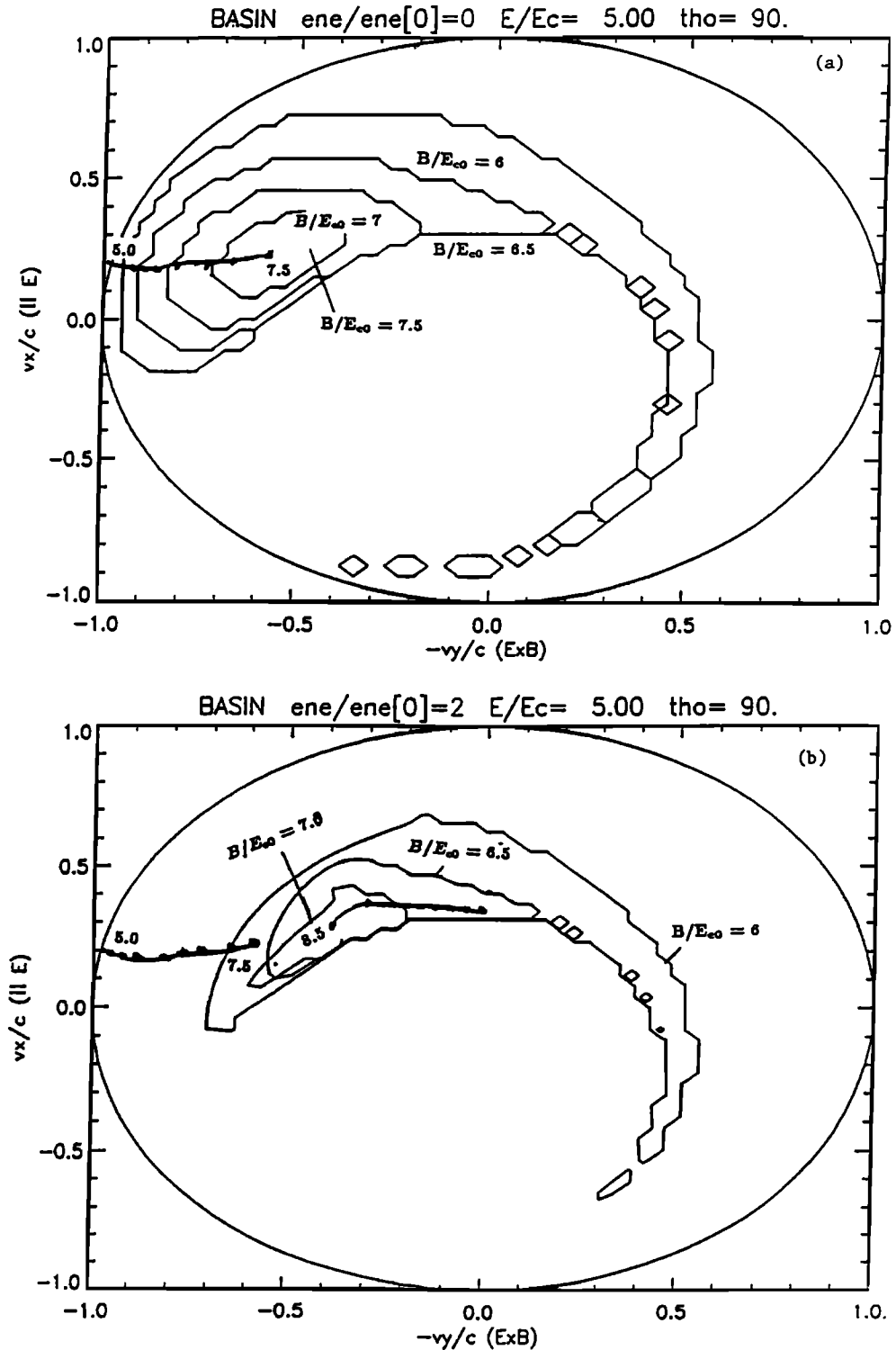


**Figure 5.** (a) Separatrix of runaway regime at  $\mathbf{E} \perp \mathbf{B}$  in the  $v_x^0/c, v_y^0/c$  plane obtained for  $\delta_0 = 5$  and  $\eta_0 = 6.0, 6.5, 7.0,$  and  $7.5$ . Separatrix of runaway breakdown. (b) Same as above except using the additional condition that the steady state kinetic energy of the runaway electron is twice as large as its initial value.

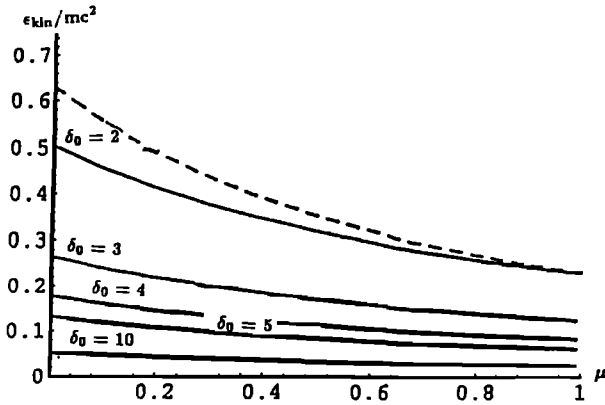


**Figure 6.** Minimum electron energy required for runaway at  $E||B$  versus the direction of the initial electron  $\mu = \cos \theta$ , obtained at  $\delta_0 = 2, 3, 4, 5$ , and  $10$ . Shown by a dashed line is the analytical approximation obtained at  $\delta_0 = 2$  [Roussel-Dupre et al., 1994].

ues of electric and magnetic fields. Note that in the absence of a magnetic field our results coincide with those obtained by Gurevich et al. [1994]. Figure 7 reveals that the magnetic field reduces the diffusion coefficient and confines the runaway discharge. The confinement is the only effect caused by the magnetic field parallel to the electric field, since the magnetic field cannot affect the electron kinetic energy.

Note that if the magnetic field is directed at a certain angle to the electric field, the runaway discharge acquires the shape of the cone having an elliptical cross section in the plane perpendicular to  $E$ . The semimajor axis is directed parallel to the projection of  $B$  on this plane, while the small semiaxis is perpendicular to this projection.

### 5. Electron Runaway Under an Arbitrary Angle Between Electric and Magnetic Fields

In a general case, when the angle  $\beta$  between the vectors  $E$  and  $B$  is  $0 < \beta < 90^\circ$ , three different ranges of the angle  $\beta$  were distinguished based on the physical properties of the runaway process. They are illustrated by the runaway trajectories shown in Figures 8a, 8b and 8c obtained for different  $\beta$ .

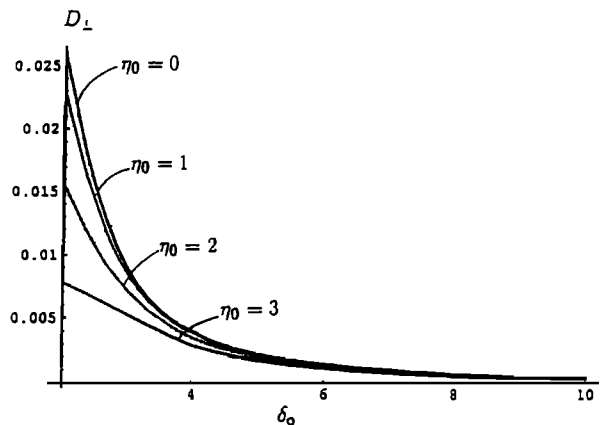
If the angle  $\beta$  ranges between  $80^\circ$  and  $90^\circ$ , the runaway process differs significantly from that which occurs in the absence of the magnetic field. First, it develops only if the ratio  $E/B$  is less than a certain threshold value, as was shown in section 2. Second, contrary to the runaway electrons in the absence of a

magnetic field where the energy gain is almost unlimited [Roussel-Dupre et al., 1994], runaway electrons at  $80^\circ < \beta < 90^\circ$  reach a steady state, at which case they orbit across the magnetic field with a constant kinetic energy, as is shown in Figure 8a obtained for  $\beta = 85^\circ$ .

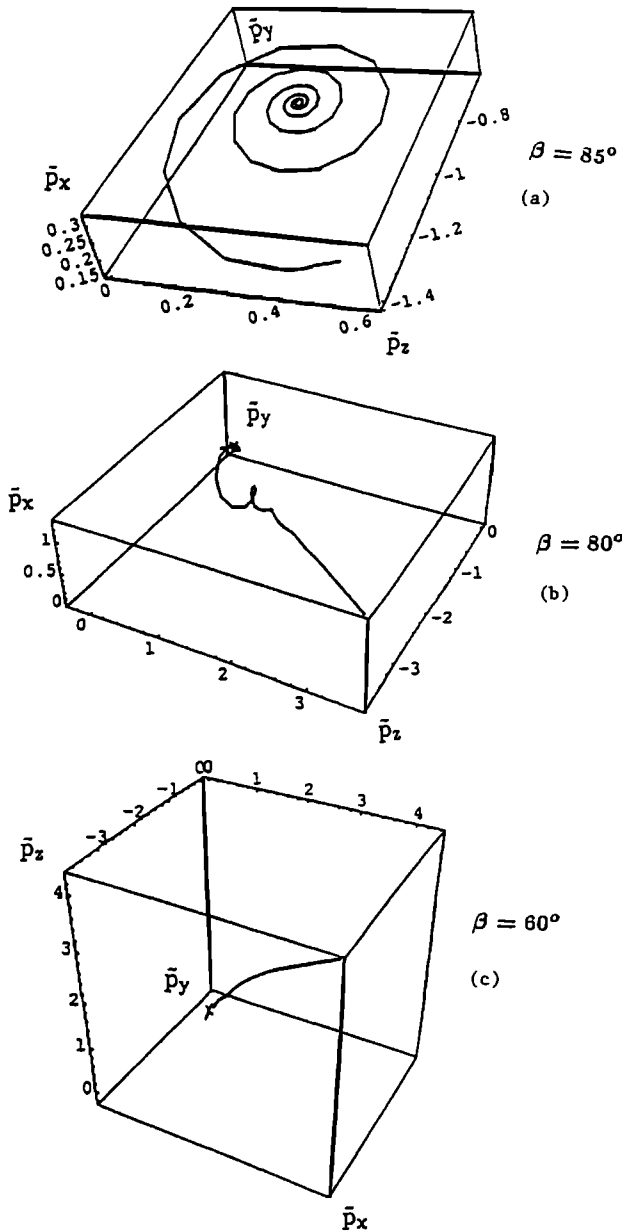
In the range of  $0^\circ < \beta < 60^\circ$  the runaway process resembles that which occurs in the absence of a magnetic field, namely, the electrons are moving along the direction of the magnetic field driven by a  $E_{||}$  component of the electric field. This is illustrated by Figure 8c, obtained at  $\beta = 60^\circ$ . The latter resembles a trajectory which is almost a straight line in the  $\tilde{p}_x, \tilde{p}_y, \tilde{p}_z$  space with a small effect of magnetic field at low momentum. However, in this case the magnetic field manifests itself by confining the runaway process, as discussed in section 4.

In the transition range  $60^\circ < \beta < 80^\circ$  the runaway electron trajectories are twisted by the magnetic field when the electrons just start acceleration and have relatively low energy. The electrons then gain energy along a straight trajectory, as shown by Figure 8b, obtained at  $\beta = 80^\circ$ .

The effect caused by the angle between the electric and magnetic fields on the runaway process is also illustrated by Figure 9, which reveals the kinetic energy of runaway electrons as a function of the angle  $\beta$ . The kinetic energy was calculated from equations (26a)-(26d) in given electric and magnetic fields, for the same initial conditions, and for the time equal to that required to reach a steady state at  $\beta=90^\circ$ . Note that  $\epsilon_{kin}(\beta = 90^\circ)/\epsilon_{kin}(\beta = 0)$  has a small but finite value; in fact, at  $\delta_0 = 5, \eta_0 = 7.5$  it is of the order of  $10^{-2}$ .



**Figure 7.** Dimensionless diffusion coefficient in the plane perpendicular to  $E||B$  obtained at  $B/E = 0, 1, 2, 3$ , and  $5$  as a function of  $\delta_0$ .



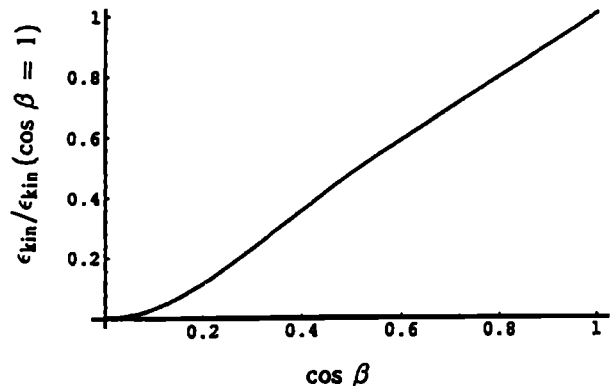
**Figure 8.** Trajectories of a runaway electron in  $\tilde{p}_x$ ,  $\tilde{p}_y$ ,  $\tilde{p}_z$  space obtained at  $\delta_0 = 5$ ,  $\eta_0 = 7.5$ , for the initial conditions  $\tilde{p}_x^0 = 0.3$ ,  $\tilde{p}_y^0 = -0.2$ ,  $\tilde{p}_z^0 = 0.2$ , and for different angle  $\beta$  between the electric and magnetic field: (a)  $\beta = 85^\circ$ , (b)  $\beta = 80^\circ$ , and (c)  $\beta = 60^\circ$ .

Figure 9 shows that at  $\cos \beta > 0.5$  (i.e.,  $\beta < 60^\circ$ ), the runaway is driven mostly by the  $E_{\parallel} = E \times \cos \beta$  component of the electric field, and it is not strongly different from that which occurred in the absence of a magnetic field, while at  $0 < \cos \beta < 0.16$  (i.e., at  $80^\circ$

$< \beta < 90^\circ$ ) the effect of the magnetic field becomes very important, and at  $0.16 < \cos \beta < 0.5$  (i.e., at  $60^\circ < \beta < 80^\circ$ ) the transition region between these two regimes exists.

The runaway boundary for an arbitrarily angle  $\beta$  could be also investigated using the following approach. We consider an ensemble of  $N_0$  electrons moving in the air in the presence of electric and magnetic fields. The electrons which are not interacting with each other are uniformly distributed in space, as well as in the energy range, which we consider for definiteness as  $1 < \gamma < 3.2$ . The trajectories of the electrons were studied using equations (26a)–(26d), and the trajectories which take electrons to higher energy were then distinguished from those which lead to zero energy. Figure 10 reveals the fraction of runaway electrons,  $N/N_0$ , as a function of  $\delta_0$ . The calculation were made for the angle  $\beta = 90^\circ$ , and from left to right, the value of  $\eta_0$  changes from 0 to 10 with step 1. In the absence of a magnetic field, shown by the left most trace, the separatrix resembles that obtained by *Roussel-Dupre et al.* [1994], while the increase of the magnetic field leads to the significant reduction in the fraction of runaway electrons.

Finally, knowing the electron runaway boundary, one can find the characteristic ionization time in the discharge caused by the runaway electrons by using the fluid approximation and assume that electron distribution function is a delta-function, i.e., consider it a monoenergetic flux of electrons. Note that of particular interest is the production rate of secondary runaway electrons, since their production leads to development



**Figure 9.** Kinetic energy of the runaway electron as a function of the angle  $\beta$ , obtained at  $\delta_0 = 5$ ,  $\eta_0 = 7$  and at initial values  $\tilde{p}_x^0 = 0.3$ ,  $\tilde{p}_y^0 = -0.2$ , and  $\tilde{p}_z^0 = 0.2$ .

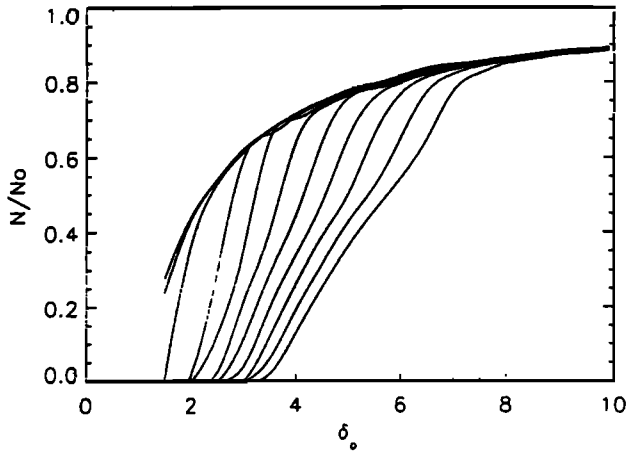


**Figure 10.** Fraction of runaway electrons as a function of the electric field  $\delta_0$  obtained for different values of the magnetic field  $\eta_0$ , at  $\beta=90^\circ$ . From left to right the value of  $\eta_0$  changes from 0 to 10 with step 1.

of the runaway breakdown. Detailed analysis of the runaway breakdown will be published elsewhere.

### 6. Discussion and Conclusions

We now state the main features regarding the behavior of runaway electrons in the constant magnetic field.

1. When the magnetic field is less than critical  $\eta_0 = B/E_{c0} < 1$ , the effect of the magnetic field on the electron runaway is almost negligible.

2. The value of the threshold electric field  $E_\eta$  required for the electron runaway in the presence of a magnetic field increases with the increase of  $\eta_0$  (see Figure 2). At a high value of  $\eta_0 \gg 1$ , the threshold field always tends to the constant value

$$E_\eta = E_{c0} / \cos \beta, \tag{34}$$

where  $\beta$  is the angle between  $\mathbf{E}$  and  $\mathbf{B}$ . This equation shows that at  $\eta_0 \gg 1$  the threshold electric field increases with  $\beta$ , which means that conditions of runaway breakdown are hindered.

3. In a case of perpendicular  $\mathbf{E}$  and  $\mathbf{B}$  fields, the value of the threshold electric field  $E_\eta$  increases smoothly with  $\eta_0$ :

$$E_\eta \approx \eta_0^{2/3} E_{c0}. \tag{35}$$

Since the critical field  $E_{c0}$  is approximately an order of magnitude less than the threshold of the conventional breakdown, it follows from equation (35) that in the case of perpendicular electric and magnetic

fields the runaway breakdown is hardly possible if  $\eta_0 \geq 30$ .

We analyze now the effect of the geomagnetic field on the runaway electrons in the atmosphere. Figure 11 reveals the critical electric field in the atmosphere along with the values of function  $\eta_0$ . The latter are given for the equatorial region where the magnetic induction is  $B_{eq} \approx 0.25$  G and for the pole region where  $B_{pol} \approx 0.6$  G. At midlatitude the function  $\eta_0$  acquires intermediate values between the two above. Figure 11 shows that critical field  $E_{c0}$  rapidly decreases with altitude. In fact, to start the runaway breakdown at the height of 30–40 km, the electric field of less than 20 V/cm will be sufficient. However, since the amplitude of the geomagnetic field is practically constant at the range of heights of interest, the value of function  $\eta_0 = B/E_{c0}$  rapidly increases with height. It comes from Figure 11 and the properties discussed above of the runaway process that for a height less than 20 km the role played by the geomagnetic field is negligible. Nevertheless, the geomagnetic field plays a noticeable role at heights which range from 20 to 30 km. In fact, it significantly changes the threshold electric field  $E_\eta$  at  $\beta \geq 45^\circ$ . At a height above 40 km the effect of the geomagnetic field dominates at large angles  $\beta$ . For instance, at  $\beta \geq 80^\circ$  the threshold electric field  $E_\eta$  increases so strongly (see equation (35) and Figure 11) that the conditions of runaway breakdown become close to those of the conventional breakdown and can be even more hindered.

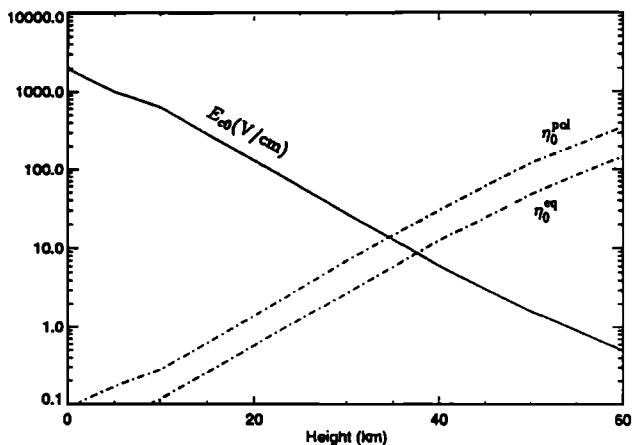


**Figure 11.** Critical field for the electron runaway  $E_{c0}$  as a function of the altitude, along with the function  $\eta_0=B/E_{c0}$ . The latter was obtained for polar and equatorial conditions,  $\eta_0^{pol}$  and  $\eta_0^{eq}$ , correspondingly.

Therefore at high altitudes  $z > 40$  km and when the angle  $\beta$  between  $\mathbf{E}$  and  $\mathbf{B}$  is close to  $\pi/2$ , the runaway breakdown is hindered, while for  $\beta \approx 0$  between  $\mathbf{E}$  and  $\mathbf{B}$  it can proceed freely. Thus, taking into consideration that the static electric field due to thunderclouds is directed almost vertically, one can expect a significant difference in the parameters of high-altitude discharges which occur in the equatorial and middle latitudes.

Finally, we obtained the runaway separatrix which separates momentum space into two regimes: those electrons which possess trajectories that take them into higher energies and other electrons which possess trajectories leading to zero energy. Using this separatrix, the characteristic ionization time required for the creation of a secondary runaway electron can be estimated.

**Acknowledgment.** The authors express their appreciation to A. S. Sharma for comments and advice. The work was supported by NSF grant ATM9422594, NASA grant NAG53117, and ISF grant M8W300.

## References

- Bell, T. F., V. P. Pasko, and U. S. Inan, Runaway electrons as a source of Red Sprites in the mesosphere, *Geophys. Res. Lett.*, **22**, 2127–2130, 1995.
- Bethe, H. A., and J. Ashkin, Passage of radiations through matter, in *Experimental Nuclear Physics*, edited by E. Segre, pp. 166–357, John Wiley, New York 1953.
- Connor, J. W., and R. J. Hastie, Relativistic limitation on runaway electrons, *Nucl. Fusion*, **15**, 415–424, 1975.
- Daniel, R. R., and S. A. Stephens, Cosmic-ray-produced electrons and gamma rays in the atmosphere, *Rev. Geophys.*, **12**, 233–258, 1974.
- Dreicer, H., Electron and ion runaway in a fully ionized gas. II, *Phys. Rev.*, **117**, 329–342, 1960.
- Fishman, G. J., et al., Discovery of intense gamma-ray flashes of atmospheric origin, *Science*, **264**, 1313–1316, 1994.
- Gurevich, On the theory of runaway electrons, *Sov. Phys. JETP, Engl. Transl.*, **12**, 904–912, 1961.
- Gurevich, A. V., G. M. Milikh, and R. Roussel-Dupre, Runaway electron mechanism of air breakdown and preconditioning during a thunderstorm, *Phys. Lett. A*, **165**, 463–467, 1992.
- Gurevich, A. V., G. M. Milikh, and R. Roussel-Dupre, Nonuniform runaway air-breakdown, *Phys. Lett. A*, **187**, 197–201, 1994.
- Lebedev, A. N., Contribution to the theory of runaway electrons, *Sov. Phys. JETP, Engl. Transl.*, **21**, 931–933, 1965.
- McCarthy, M. P., and G. K. Parks, On the modulation of X ray fluxes in thunderstorms, *J. Geophys. Res.*, **97**, 5857–5864, 1992.
- Roussel-Dupre, R., and A. V., Gurevich, On runaway breakdown and upward propagating discharges, *J. Geophys. Res.*, **101**, 2297–2311, 1996.
- Roussel-Dupre, R., A. V. Gurevich, T. Tunnel, and G. M. Milikh, Kinetic theory of runaway air breakdown, *Phys. Rev. E*, **49**(3), 2257–2271, 1994.
- Uman, M. A., *The Lightning Discharge*, Academic, San Diego, Calif., 1987.
- Wilson, C. T. R., The acceleration of  $\beta$ -particles in strong electric fields such as those of thunderclouds, *Proc. Cambridge Philos. Soc.*, **22**, 534–538, 1924.

---

A. V. Gurevich, G. M. Milikh, K. Papadopoulos, and J. A. Valdivia, Department of Astronomy, University of Maryland, College Park, MD 20742–2421. (e-mail: milikh,@avl.umd.edu; kp@spp.umd.edu)

(Received March 4, 1996; revised July 24, 1996; accepted August 9, 1996.)